

B-1-7

## Influence on Electrical Characteristic of Direct Au-Bumping on MOSFET

Naoya Watanabe and Tanemasa Asano

Center for Microelectronic Systems, Kyushu Institute of Technology

680-4 Kawazu, Iizuka, Fukuoka 820-8502, Japan

Phone: +81-948-29-7589, Fax: +81-948-29-7586, E-mail: naoya@cms.kyutech.ac.jp

### 1. Introduction

The area bump technology can greatly facilitate signal processing speed and function of LSIs. This is because it allows to form a very high number of I/O connections in a chip, and to integrate LSI chips using a full-surface flip-chip interconnection which will realize three dimensional chip integration even with heterogeneous chips. Au is the most reliable bump material since it is inert and bumps can be formed at low temperature with the aid of ultrasonic vibration. The Au area-bump formation on active devices, however, causes change in characteristic of devices because strain is generated during the application ultrasonic vibration. It has been reported that Au bump formation on MOSFETs causes an increase in gate-SiO<sub>2</sub>/Si interface states [1]. Further investigation is needed to clarify which stage of Au-bump formation process is critical and why electrical characteristic changes.

We have succeeded to detect dynamic strain and its distribution generated at the surface of Si under an Au bump during ultrasonic bump formation [2]. In this work, in conjunction with the dynamic strain measurement, influence of Au-bump formation directly on MOSFETs on electrical characteristic of MOSFETs is investigated. It is found that the residual strain changes the transconductance  $g_m$  of MOSFETs, nevertheless the fact that much higher dynamic strain is generated during the application of ultrasonic vibration than the residual strain.

### 2. Experimental

In order to measure dynamic strain generated during Au bump formation and change in electrical characteristic of MOSFET, arrays of strain gauges and MOSFETs were fabricated. Figure 1(a) shows an optical micrograph of a MOSFET array. The array contains 5 MOSFETs. W/L of each MOSFET was 20  $\mu\text{m}$ / 5  $\mu\text{m}$ . The interval between MOSFETs was 20  $\mu\text{m}$ , which are small enough to measure the distribution of change in device characteristic under a bump ( $\simeq$  90  $\mu\text{m}$  in diameter). Arrays of n-channel and p-channel MOSFETs were fabricated. The thickness of gate oxide was 30 nm. The channel direction of MOSFETs was aligned with either  $\langle 110 \rangle$  or  $\langle 100 \rangle$  direction on (100) substrates to investigate effects of strain on MOSFET performance. Two Al layers (first layer: 500 nm-thick, second layer: 1000nm layer-thick) were formed: The first layer is for electrical interconnection and the second layer is for bonding pad. The interlayer dielectric was 500 nm-thick PECVD SiO<sub>2</sub>. The arrays of Si-piezoresistive strain gauges having 20  $\mu\text{m}$  spatial resolution were fabricated by similar manner to the MOSFET arrays.

An Au bump was formed directly on a MOSFET ar-

ray and on a strain gauge array. The relative position between the MOSFET array and the bump is shown in Fig. 1(b). Bonding condition was as follows, ultrasonic frequency: 60 kHz, ultrasonic power: 150 mW, ultrasonic time: 20 msec, pressing force: 90 gf, chip temperature: 120 °C. The spatial distribution of change in MOSFET characteristics and that of both dynamic and residual strains were measured.

### 3. Results and Discussion

Change in  $V_{th}$  of MOSFETs before and after Au bumping was only a few mV for both n- and p-channel MOSFETs. This suggests that no significant generation of charge state occurs even an Au bump is formed directly on MOSFETs. On the other hand, there appeared slight change in transconductance  $g_m$  of MOSFET, which was dependent on the relative position between MOSFET and the bump. Figure 2 shows the spatial distribution of the maximum  $g_m$  change ( $\Delta g_m/g_{m0}$ ) after Au bumping, where  $g_{m0}$  and  $\Delta g_m$  are initial  $g_m$  value and the change from its initial value after bumping, respectively. We can find that (1) change in  $g_m$  is maximum at the center of the bump and its value is a few %, and (2) direction of change is symmetrical between n-channel and p-channel.

The spatial distribution of the of  $g_m$  change was compared with that of ultrasonic strain and residual strain measured with strain gauge array. Figure 3 shows an example of strain time-evolution during Au bump formation. We can see the strain at the pre-press step, large oscillating strain at the ultrasonic step, and the residual strain. Figures 4(a) and 4(b) show spatial distribution of strain generated during ultrasonic application and residual strain, respectively. The strain shown in Fig. 4(a) is RMS value of the oscillating strain. The dynamic (oscillating) strain has the maximum near the periphery of the bump, while the residual strain has the maximum near the center of the bump. These results suggest that the  $g_m$  change is caused not by the ultrasonic strain but by the residual strain.

To ascertain the influence of residual strain, we measured the strain dependence of  $\Delta g_m/g_{m0}$  by applying bending deformation to MOSFET chip. Figure 5 shows the strain dependence of  $\Delta g_m/g_{m0}$  observed for n- and p-channel MOSFET. Through these results, the observed  $g_m$  changes (Fig. 2) can be quantitatively correlated with the residual strain (Fig. 4(b)). This indicates that the  $g_m$  change is due to piezoresistive effect [3] of residual strain.

Further investigation was carried out by aligning the MOSFET direction with  $\langle 100 \rangle$  on (100) substrate. In

Fig. 6, changes in  $g_m$  of p-channel MOSFETs whose channel directions were  $\langle 110 \rangle$  or  $\langle 100 \rangle$  were plotted. We find that the  $g_m$  change is smaller for MOSFETs aligned with  $\langle 100 \rangle$  than for those aligned with  $\langle 110 \rangle$ . This result agrees well with fact that, for hole transportation, the piezoresistive coefficient is smaller for  $\langle 100 \rangle$  direction than  $\langle 110 \rangle$  direction.

#### 4. Conclusion

Influence on electrical characteristics of MOSFET of direct Au-bump formation on the MOSFET have been investigated. In spite of the fact that a relatively large dynamic strain is generated during the application of ultrasonic vibration, only the residual strain causes a change in transconductance. The bump formation does not significant affect  $V_{th}$ . The results will contribute to development of area bump technology for advanced system integration.

#### Acknowledgment

This work was supported in part by the Grant-in-Aid for Scientific Research (No. 13025239) from the Ministry of Education, Culture, Sports, Science and Technology.

#### References

- [1] N. Shimoyama, et al: Ext. Abs. 1998 Int. Conf. SSDM (1998) p. 88.
- [2] M. Hizukuri and T. Asano: Jpn. J. Appl. Phys. Vol. 39 (2000) p. 2478.
- [3] C.S. Smith : Phys. Rev. Vol. 94 (1954) p. 42.

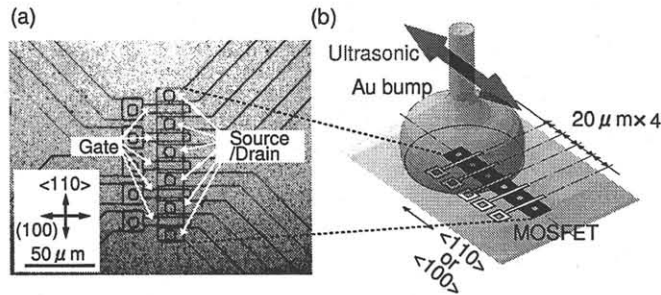


Fig. 1: (a) Optical micrograph of a MOSFET array. (b) The relative position between the MOSFET array and the bump.

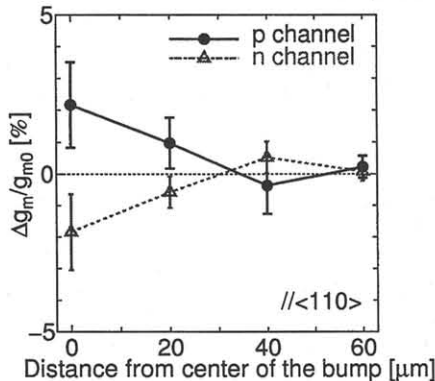


Fig. 2: The distribution of the maximum  $g_m$  change ( $\Delta g_m/g_{m0}$ ) due to Au bumping. The channel was aligned with  $\langle 110 \rangle$  on Si(100).

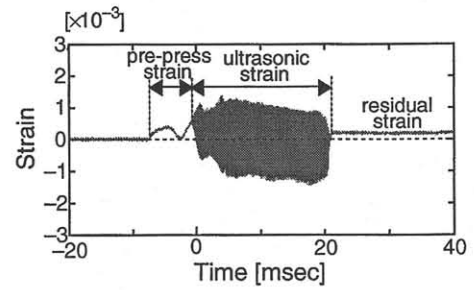


Fig. 3: An example of strain time-evolution during Au bump formation.

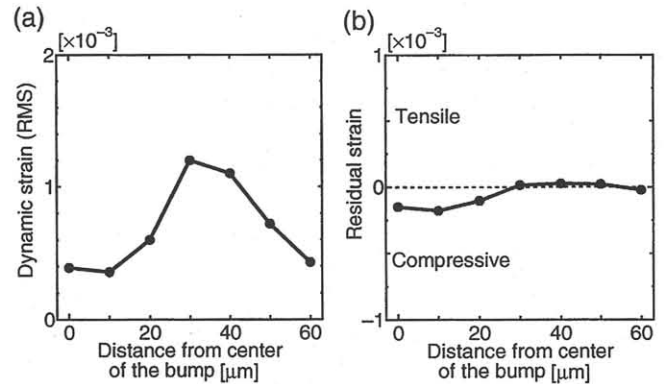


Fig. 4: (a) The distribution of the dynamic strain during application of the ultrasonic vibration to the bump. The vertical axis shows the root mean square of the strain. (b) The distribution of the residual strain observed after Au bumping.

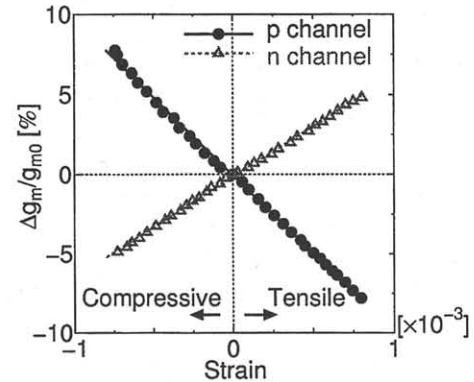


Fig. 5: The strain dependence of  $\Delta g_m/g_{m0}$ .

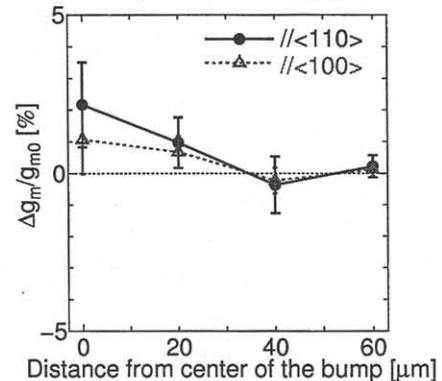


Fig. 6: Change in  $g_m$  of pMOSFETs whose channel was aligned with  $\langle 110 \rangle$  or  $\langle 100 \rangle$ .